Title: Metformin reduces left ventricular eccentric remodeling in experimental volume overload in the rat.

Wahiba Dhahri, Élise Roussel, Marie-Claude Drolet, Suzanne Gascon§, Otman Sarrhini§, Jacques A. Rousseau§, Roger Lecomte§, Jacques Couet* and Marie Arsenault*

Groupe de Recherche en Valvulopathies, Centre de Recherche, Institut universitaire de cardiologie et de pneumologie de Québec, Université Laval, Québec, Canada.

§: Centre d'imagerie moléculaire de Sherbrooke, Centre de recherché Étienne-LeBel, Centre Hospitalier Universitaire de Sherbrooke, Université de Sherbrooke, Sherbrooke, Canada.

Running head: Effects of metformin on eccentric left ventricular hypertrophy

*: Corresponding authors: Jacques Couet PhD or Marie Arsenault MD

Groupe de Recherche en Valvulopathies, Centre de Recherche,

Institut universitaire de cardiologie et de pneumologie de Québec

2725, Chemin Sainte-Foy, Quebec City, QC, Canada, G1V 4G5

Phone: 1-418-656-4760; Fax: 1-418-656-4509

Email: jacques.couet@med.ulaval.ca or marie.arsenault@criucpq.ulaval.ca

Abstract

Aims: Left ventricular hypertrophy (LVH) is often associated with a change in myocardial energy substrate preference from fatty acids to glucose. A possible antihypertrophic treatment strategy could aim at stimulating or restoring normal myocardial energy metabolism. Metformin, an adenosine monophosphate-activated protein kinase (AMPK) activator used in the management of glucose metabolism in diabetes, is also a fatty acid oxidation stimulator. The effect of metformin on the development of eccentric LVH and ventricular function in chronic left ventricular (LV) volume overload (VO) is unknown. This study was designed to study this question in a VO rat model caused by severe aortic valve regurgitation (AR).

Methods: Male Wistar rats were divided in four groups (13-15 animals / group): Shams (S) treated or not (C) with metformin (M; 100 mg/kg/d PO) and severe AR receiving or not metformin. Treatment was started one week before surgery and the animals were sacrificed 9 weeks later.

Results: As expected AR rats developed severe eccentric LVH during the course of the protocol. Metformin treatment did not influence the total heart weight. However, LV remodeling associated with the severe VO was severe in ARM than in ARC. Fractional shortening, a marker of systolic function, was significantly higher in ARM compared to ARC group. Metformin also increased the activity of enzymes associated with fatty acid oxidation while inhibiting phosphofructokinase, a glycolytic enzyme.

Conclusion: A 2 month treatment with metformin reduced LV eccentric remodeling associated with severe VO and helped maintain a better systolic function.

Key words: cardiomyopathy, volume overload, metformin, hypertrophy

Introduction

Chronic left ventricular volume overload (VO) causes severe left ventricular dilatation and eccentric hypertrophy (LVH). LVH causes alterations in myocardial energy metabolism. The normal myocardium has a preference for fatty acids as the main substrate for ATP formation. In the hypertrophied heart, an increased reliance on glucose with an overall reduced oxidative metabolism is often observed [1-3]. Impaired myocardial energetics also activate AMP-activated protein kinase (AMPK), leading to increased glucose uptake and glycolysis [4]. AMPK activation can also stimulate fatty acid oxidation and block the mammalian target of rapamycin (mTOR) pro-hypertrophic pathway [5]. Metformin is an AMPK activator widely used for the management of type 2 diabetes but its potential to help maintain normal myocardial metabolism and/or prevent LVH is not well understood [6]. We have previously demonstrated that LV volume overload caused by aortic valve regurgitation causes severe eccentric LVH and also significantly impairs myocardial metabolism [7].

This study was therefore designed to assess the impact of a treatment with an AMPK activator, metformin, on the development of eccentric LVH from volume overload from severe AR in Wistar rats.

Methods

Animals: The animal protocol design was a 2 x 2 type study where animals were surgically induced with the aortic valve lesion of only sham-operated and then received or not the metformin treatment. Adult male Wistar rats were purchased from Charles River (Saint-Constant QC, Canada) and divided in 4 groups as follows: 1) Sham-operated animals (SC; n=14); 2) AR (ARC; n=15), 3) Sham treated with metformin (M) (150 mg/kg/d PO in unsweetened fruit gelatin; SF; n=14) and AR on metformin (ARM n=15). The treatment was started one week before surgery in both S and AR groups and continued for 9 weeks until sacrifice. The animals were housed in a 12 hr light/dark cycle. Access to food and water was free. The protocol was approved by the Université Laval's Animal Protection Committee and followed the recommendations of the Canadian Council on Laboratory Animal Care.

Aortic regurgitation: Severe AR was induced by retrograde puncture of the aortic valve leaflets as previously described [8, 9]. A complete echocardiographic exam was performed two weeks after AR induction and the day before sacrifice 8 weeks later. At the end of the protocol, animals were sacrificed, hearts were quickly dissected and all cardiac chambers were weighed. LV was snap-frozen in liquid nitrogen and kept at -80^{o}C for further analysis. All sacrifices were scheduled at similar times of the day in the fed state to avoid circadian variations in metabolism. Lungs, liver and abdominal fat were rapidly collected and weighed.

Echocardiography

A complete M-mode, 2D, and Doppler echocardiogram was performed on the animals under 1.5% inhaled isoflurane anesthesia using a 12 MHz probe with a Sonos 5500 echograph (Philips Medical Imaging, Andover, Mass). LV dimensions, wall thickness, ejection fraction, cardiac output (ejection volume in the LV outflow tract and heart rate) were evaluated as previously reported [10-12].

Small animal PET protocol: Imaging experiments and data analysis were performed essentially as described before [13-16] on a LabPET™ avalanche photodiode-based small animal PET scanner (Gamma Medica, Northridge, CA) at the Sherbrooke Molecular Imaging Centre. [^{18}F]-fluorodeoxyglucose ([^{18}F]-FDG), [^{18}F]-fluorothioheptadecanoic acid ([^{18}F]-FTHA) or [^{11}C]-acetate(30–40 MBq, in 0.3 ml plus 0.1 ml flush of 0.9% NaCl, respectively) was injected via the caudal vein over 30 s. In one set of experiments, a 10-min dynamic acquisition with [11C]acetate and a 45-min dynamic acquisition with [18F]FDG were done to determine myocardial oxidative metabolism [O2 uptake (V̇o2)] and glucose utilization [myocardial metabolic rate of glucose (MMRG)]. In another experiment, a 45-min dynamic acquisition with [18F]FTHA was used to determine myocardial non-esterified fatty acid (NEFA) uptake (Km) [14]. Blood samples were taken before and after the scans to determine an average blood glucose level. Image data analysis was performed as described previously [15]. Myocardial NEFA fractional uptake (Ki) was determined by a Patlak graphical analysis of the [18F]FTHA data [14]. For [11C]acetate, we used a three-compartment kinetic model that estimates the generation of CO2 from the citric acid cycle in the myocardium using the k2 value [16]. The myocardial metabolic rate of glucose (MMRG) was determined by multicompartmental analysis of the [18F]FDG data [13,14].

Analysis of mRNA accumulation by quantitative RT-PCR

The analysis of LV mRNA levels by quantitative RT-PCR has been described in details elsewhere [17]. Briefly, one µl RNA (500 ng) was converted to cDNA using the QuantiTect Reverse Transcription kit (Qiagen, Valencia, CA). The cDNA obtained was further diluted 11-fold with water prior to amplification. Five µl of diluted cDNA were amplified in duplicate by Q-PCR in a Rotor-Gene thermal cycler (Corbett Life Science. Sydney, Australia), using QuantiTect Primer Assays (pre-optimized specific primer pairs from Qiagen) and QuantiFast® SYBR Green PCR kits (Qiagen). Cyclophilin A as an housekeeping gene was used as a control. In Table 1, the list of primers used in this study is illustrated.

Enzyme activity determinations

Left ventricle samples were kept at -80°C until assayed for maximal (V_{max}) enzyme activities. Small pieces of LV (20-30mg) were homogenized in a glass-glass homogenizer with 9 or 39 volumes of ice-cold extracting medium pH7.4 (250mM sucrose, 10mM Tris-HCl, 1mM EGTA) depending on the enzyme activity assayed. Enzymatic activities for hydroxyacyl-Coenzyme A dehydrogenase (HADH), phosphofructokinase (PFK) and citrate synthase (CS) were determined as previously described [7].

Immunoblotting

Crude LV homogenates were separated by SDS-PAGE. Volumes of samples loaded on gel were corrected for the amount of protein. Immunoblotting was performed as

described elsewhere [18]. Membranes were hybridized with the indicated primary antibodies. All primary antibodies against the phosphorylated or the total form of the different signaling proteins (Erk 1/2, p38, Jnk, AMP kinase, LKB1 and Akt) were used at a 1:1000 dilution and were purchased from Cell Signaling Technology (Beverly, MA). Bands were visualized and quantified with a ChemiImager system (Alpha Innotech Corporation).

Statistical analysis

Results are presented as mean ± SEM unless specified otherwise. Inter-group comparisons were done using two-way ANOVA and using Bonferroni post-test if necessary. Student t-test was used when two groups were compared head to head. Statistical significance was set at a $p<0.05$. Data and statistical analysis were performed using Graph Pad Prism version 5.02 for Windows, Graph Pad Software (San Diego CA).

Results

Increased myocardial glucose and decreased fatty acid uptake in AR rat myocardium (Figure 1).

We compared using μPET imaging the glucose and fatty acid uptake of left ventricles of AR animals 8 weeks post-induction to sham-operated animals. As illustrate in Figure 1, glucose uptake was increased in AR rats while fatty acid uptake was decreased. Interestingly, despite these changes, myocardial oxygen consumption remained normal between groups.

Clinical data and animal characteristics (Table 2):

At the end of the protocol, all animals were alive with the exception of one in the ARC group. Body weight and tibial length were equivalent in all experimental groups (Table 2). Total heart weight was greatly increased in rats with AR. Metformin had no effect on this parameter. The weight of both left and right ventricles were markedly increased in AR animals but again metformin had no effect on the weight of both ventricles respectively.

Echocardiographic LV remodeling and hemodynamic data (Table 3 and Figure 3):

End-diastolic and end-systolic LV dimensions were increased in AR animals as expected (Table 3). Metformin treatment reduced both systolic and diastolic LV dilatation in AR as shown by the reduced diastolic and systolic diameter in ARM vs. ARC group. Wall thicknesses were increased in the ARM group vs. ARC but similar to the shams treated with metformin. Relative wall thickness (RWT) was therefore normalized in ARM

thereby confirming less eccentric remodeling in animals treated with metformin. Interestingly, RWT also increased in sham-operated animals on metformin suggesting that the drug has an impact on LV remodeling even in normal animals. As illustrated in Figure 2 in transaxial LV sections, AR was associated with larger LVs and metformin seemed to increase wall thickness. Systolic function evaluated by fractional shortening was clearly improved in ARM animals compared to the ARC. ARM rats had a lower (closer to normal) stroke volume in this group and a closer to normal calculated cardiac output (Figure 3). Pulse pressure increased in both ARM and ARC groups as expected and metformin did not have any effect on this parameter (results not shown).

Markers of LV stress and hypertrophy (Figure 4).

As expected, ANP and BNP expressions in LV myocardium were increased in AR animals as a result of the important pro-hypertrophic hemodynamic stress caused by AR. Metformin did not decrease the level of expression of ANP or BNP. A similar pattern of expression was also observed for the endothelin-1 mRNA. Fos expression is also usually associated with hypertrophy in the myocardium. As expected, the level of Fos expression was increased by AR groups. Metformin treatment was associated with a strong trend to decrease Fos expression in ARM animals. This decrease in Fos expression by metformin was also present in the sham animals.

Myocardial extracellular matrix remodeling (Figure 5)

The expression of various markers involved in myocardial fibrosis was evaluated in LV myocardium. AR increased the expression of collagen III and IV as well as Lox and TGFβ and fibronectin. The expression of collagen I remained normal in ARC. The

expression of MMP2 and TIMP1 were also increased by AR. Metformin treatment in AR increased the expression of collagen I and III as well as fibronectin. It also tended to increase TIMP1 expression. However, we found no increase in fibrosis on direct LV tissue Trichrome-Masson staining (results not shown).

Myocardial metabolism

Eight weeks after AR induction, changes in energy substrate uptake are observed in the myocardium as illustrated in Figure 1. We measured the activity levels of various metabolic enzymes in LV tissue of all groups. Results are shown in Figure 6. The HADH (hydroxyacyl-Coenzyme A dehydrogenase) responsible for fatty acid β-oxidation was less active in the AR group after 8 weeks compared to sham animals. Metformin treatment had no effect on this parameter. The first step of glycolysis is catalyzed by the hexokinase (HK). HK activity levels were significantly increased in all AR animals compared to the shams and metformin further increased this activity. The entry of acetyl-CoA in the citric acid cycle is catalyzed in the mitochondria by the citrate synthase (CS). CS activity levels were however significantly lower in AR animals. Metformin treatment increased CS activity levels in the LV of both sham and AR animals.

With the exception of Glut1 mRNA expression, metformin treatment did not modulate other genes related with the control of energy metabolism tested in this protocol (Figure 7). Interestingly, the majority of them were down-regulated in AR animals.

Metformin treatment impact on signaling in AR rats.

We measured the ratio of the phosphorylated form on the total content of a number of signaling molecules implicated in both hypertrophic and energy metabolism pathways. As illustrated in Figure 8, activated Erk1/2 and Jnk1/2 are more abundant in AR LVs compared to sham-operated ones. Metformin treatment was associated with a decrease in the content of phosphorylated forms of p-38 and Jnk1/2 and an expected increase was observed for the AMP kinase.

Discussion

This study shows that an 8-week treatment with metformin reduces eccentric LV remodeling and dilatation in an experimental model of volume overload caused by severe aortic valve regurgitation. Metformin also helped maintain systolic function (ejection fraction). It also increased the activity of metabolic enzymes HK and CS. The treatment was not powerful enough however to prevent LV hypertrophy. This was expected considering the acute severe stress imposed to the LV. The fact that metformin was able to reduce LV dilatation and eccentric remodeling under such acute stress conditions, is in itself remarkable and exciting. In line with the law of Laplace, we can suppose that wall stress was reduced in AR rats treated with metformin (less dilatation and thicker walls). Our results show that metformin has the potential to act as a protector of the LV in volume overload. Long term studies will answer the question whether this hypothesis remains true over time.

The main mechanism of action of metformin is believed to be via the activation of the AMPK [6]. Metformin does not bind directly to AMPK. One hypothesis is that it inhibits the respiratory chain Complex I causing an increase in the AMP/ATP ratio [19]. In our study, metformin treatment led to AMPK activation. After 8 weeks, AMPK levels of activation were similar to controls in the LV of AR rats. On the other hand, LKB1 phosphorylation was reduced in AR rats and metformin restored normal levels of LKB1 activation. LKB1 is a known AMPK kinase together with the calmodulin-dependent protein kinase kinase (CamKK) which is expressed only at low levels in cardiac myocytes but other kinases have also been proposed to be responsible for the metformin-induced phosphorylation of the AMPK such as PKCζ [20]. It has also been

shown the metformin can exert beneficial metabolic effect independently from the AMPK in cardiac myocytes presumably via p38 or PKC-related signaling [21].

Metformin has been reported to decrease hypertrophy and slow the onset of heart failure in several animal models [22-24].

Cardiac hypertrophy is associated with the reappearance of a “fetal profile” of gene expression. We observed such a “fetal profile” in this study and previous ones using our AR model after a longer follow-up (> 6 months) with a modification in the expression of heart myosin heavy chains subtypes [12] and increased expression of Glut 1 and c-Fos. This profile is associated with increased glucose utilization and was at first considered maladaptive [4]. The observation that cardiac overexpression of GLUT1 prevented the development of heart failure (and LV dilation) attributable to pressure overload in mice with little effects on overall LVH changed this perception [25]. It is now believed that glucose reliance in the adult heart is not harmful while reduced ability to utilize glucose could be detrimental in cardiac hypertrophy or heart failure [4]. In our study metformin treatment was associated with an increased expression of Glut1 and a raised activity of the hexokinase in AR animals with an already augmented glucose uptake in AR animals. Increased AMPK activity was shown to promote the translocation of the glucose transporters [26].

It is not clear how metformin (via AMPK activation or not) can modulate LV remodeling caused by severe chronic VO. In a recent study in a model of global heart volume overload caused by aortocaval fistulae (ACF) in rats, metformin was shown to have no impact on the heart and LV weight in ACF rats while echo data showed a trend similar to ours (less dilatation). In that study the dose of metformin was twice the one we used

(27). In another study in rats post-myocardial infarction, metformin was shown to decrease heart dilatation while limiting LV wall thinning [28].

We observed that metformin decreased the protein content of the phosphorylated forms of both stress kinases p38 and Jnk. Both kinases have been shown in the past to have pro-hypertrophic action [29]. Inhibition of p38 in H9C2 cells was shown to decrease glycolysis [21]. Metformin has also been shown to inhibit Jnk activation in the past (Jung BBRC 2012). It is not clear whether metformin is acting on LV remodeling in our model via the inhibition of these pathways.

Metformin was shown in the past to slow the development of myocardial interstitial fibrosis [28]. Interstitial fibrosis is usually less present in VO-induced hypertrophy than in pressure overload situations. We have shown in the past that LV collagen content is still normal after 8 weeks in AR rats even though gene expression of many extracellular matrix (ECM) components is increased [10]. Here we observed that metformin further increased collagen type I and III gene expression in AR LVs. A trend for a higher expression of other ECM components was also present in metformin-treated animals. This suggests that metformin treatment could be associated with a higher turnover of ECM proteins. However this may also be an early sign of increased myocardial fibrosis in a more chronic state. Longer studies will be necessary to better characterize this observation.

The results of this study have to be viewed in light of some limitations. This was a relatively short study in which metformin was given as a pre-disease treatment. Eight weeks may be too short to assess the impact of metformin treatment on systolic and diastolic functions and clinical evolution on the long term. Rodent heart metabolism may also differ in some aspects from humans.

In conclusion, metformin treatment is associated with less eccentric remodeling, less LV dilatation and a better systolic function in an experimental model of LV volume overload caused from aortic valve regurgitation. Long term studies evaluating the effects of such treatment on LV function and survival are mandated.

Acknowledgements: This work was supported by operating grants to Dr Couet and Arsenault from the Canadian Institutes of Health Research (MOP-61818 and MOP-106479) and the Quebec Heart Institute Corporation.

References

1. Allard MF (2004) Energy substrate metabolism in cardiac hypertrophy. Curr Hypertens Rep 6: 430-435.

2. Allard MF, Parsons HL, Saeedi R, Wambolt RB, Brownsey R (2007) AMPK and metabolic adaptation by the heart to pressure overload. Am J Physiol Heart Circ Physiol 292: H140-H148.

3. Sambandam N, Lopaschuk GD, Brownsey RW, Allard MF (2002) Energy metabolism in the hypertrophied heart. Heart Fail Rev 7:161-173.

4. Kolwicz Jr SC, Tian R (2011) Glucose metabolism and cardiac hypertrophy. Cardiovas Res 90: 194-201.

5. Hardie DG (2004) The AMP-activated protein kinase pathway – newplayers upstream and downstream. Journal of Cell Science 117: 5479-5487.

6. Wong, AKF, Howie J, Petrie JR, Lang CC (2009) AMP-activated protein kinase pathway: a potential therapeutic target in cardiometabolic disease. Clin Sci (Lond) 116: 607-620.

7. Bouchard-Thomassin AA, Lachance D, Drolet MC, Couet J, et al (2011) A high fructose diet worsens eccentric left ventricular hypertrophy in experimental volume overload. Am J Physiol Heart Circ Physiol 300: H125-134.

8. Arsenault M, Plante E, Drolet MC, Couet J (2002) Experimental aortic regurgitation in rats under echocardiographic guidance. J Heart Valve Dis 11: 128-34.

9. Plante E, Couet J, Gaudreau M, Dumas MP, Drolet MC, et al. (2003) Left ventricular response to sustained volume overload from chronic aortic valve regurgitation in rats. J Card Fail 9:128-140.

10. Lachance D, Plante E, Bouchard-Thomassin AA, Champetier S, Roussel E, et al (2009) Moderate exercise training improves survival and ventricular remodeling in an animal model of left ventricular volume overload. Circ Heart Fail 2: 437-445.

11. Plante E, Lachance D, Beaudoin J, Champetier S, Roussel E, et al. (2009) Comparative study of vasodilators in an animal model of chronic volume overload caused by severe aortic regurgitation. Circ Heart Fail 2: 25-32.

12. Plante E, Lachance D, Champetier S, Drolet MC, Roussel E, et al. (2008) Benefits of long-term {beta}-blockade in experimental chronic aortic regurgitation. Am J Physiol Heart Circ Physiol 294: H1888-H1895.

13. Ménard SL, Ci X, Frisch F, Normand-Lauzière F, Cadorette J, et al. (2009) Mechanism of reduced myocardial glucose utilization during acute hypertriglyceridemia in rats. Mol Imaging Biol 11:6-14.

14. Ménard SL, Croteau E, Sarrhini O, Gélinas R, Brassard P, et al. (2010) Abnormal in vivo myocardial energy substrate uptake in diet-induced type 2 diabetic cardiomyopathy in rats. Am J Physiol Endocrinol Metab 298:E1049-E1057.

15. Croteau E, Bénard F, Cadorette J, Gauthier ME, Aliaga A, et al. (2003) Quantitative gated PET for the assessment of left ventricular function in small animals. J Nucl Med 44:1655-1661.

16. Croteau E, Gascon S, Bentourkia M, Langlois R, Rousseau JA, et al. (2012) [^{11}C]Acetate rest–stress protocol to assess myocardial perfusion and oxygen

consumption reserve in a model of congestive heart failure in rats. Nucl Med Biol. 39:287-294.

17. Champetier S, Bojmehrani A, Beaudoin J, Lachance D, Plante E, et al. (2009) Gene profiling of left ventricle eccentric hypertrophy in aortic regurgitation in rats: rationale for targeting the beta-adrenergic and renin-angiotensin systems. Am J Physiol Heart Circ Physiol 296:H669-H677.

18. Plante E, Lachance D, Gaudreau M, Drolet MC, Roussel E, et al. (2004). Effectiveness of beta-blockade in experimental chronic aortic regurgitation. Circulation 110: 1477-1483.

19. Owen MR, Doran E, Halestrap AP (2000) Evidence that metformin exerts its anti-diabetic effects through inhibition of complex 1 of the mitochondrial respiratory chain. Biochem J 348: 607-614.

20. Ussher JR, Jaswal JS, Wagg CS, Armstrong HE, Lopaschuk DG, et al. (2009) Role of the atypical protein kinase Czeta in regulation of 5'-AMP-activated protein kinase in cardiac and skeletal muscle. Am J Physiol Endocrinol Metab 297: E349-E357.

21. Saeedi R, Parsons HL, Wambolt RB, Paulson K, Sharma V, et al. (2008) Metabolic actions of metformin in the heart can occur by AMPK-independent mechanisms. Am J Physiol Heart Circ Physiol 294: H2497-H2506.

22. Gundewar S, Calvert JW, Jha S, Toedt-Pingel I, Ji SY, et al. (2009). Activation of AMP-Activated Protein Kinase by Metformin Improves Left Ventricular Function and Survival in Heart Failure. Circ Res 104: 403-411.

23. Sasaki H, Asanuma H, Fujita M, Takahama H, Wakeno M, et al. (2009) Metformin prevents progression of heart failure in dogs: role of AMP-activated protein kinase. Circulation 119: 2568-2577.

24. Zhang CX, Pan SN, Meng RS, Peng CQ, Xiong ZJ, et al. (2011) Metformin attenuates ventricular hypertrophy by activating the AMP-activated protein kinase-endothelial nitric oxide synthase pathway in rats. Clin Exp Pharmacol Physiol. 38: 55-62.

25. Liao R, Jain M, Cui L, D'Agostino J, Aiello F, et al. (2002) Cardiac-specific overexpression of GLUT1 prevents the development of heart failure attributable to pressure overload in mice. Circulation 106: 2125-2131.

26. Nascimben L, Ingwall JS, Lorell BH, Pinz I, Schultz V, et al. (2004) Mechanisms for increased glycolysis in the hypertrophied rat heart.Hypertension 44: 662-667.

27. Benes J, Kazdova L, Drahota Z, Houstek J, Medrikova D, et al. (2011) Effect of metformin therapy on cardiac function and survival in a volume-overload model of heart failure in rats. Clin Sci (Lond) 121: 29-41.

28. Yin M, van der Horst IC, van Melle JP, Qian C, van Gilst WH, et al. (2011) Metformin improves cardiac function in a nondiabetic rat model of post-MI heart failure. Am J Physiol Heart Circ Physiol 301: H459-H468.

29. Liang Q, Molkentin JD (2003) Redefining the roles of p38 and JNK signaling in cardiac hypertrophy: dichotomy between cultured myocytes and animal models. Journal of Molecular and Cellular Cardiology 35: 1385–1394.

Figure legends:

Figure 1: Myocardial glucose (top) and fatty acid (middle) uptakes as well as oxidative metabolism (bottom) modulation in the LV myocardium of AR rats as evaluated by µPET. Myocardial rate of glucose (MMRG) and FTHA uptake and myocardial oxidative metabolism using acetate were evaluated as described in the Materials and Methods section in both sham-operated and AR rats 8 weeks post-surgery (n=4/gr.) and are expressed as the mean ± SEM. P values were calculated using the student t-test.

Figure 2: Typical macroscopic examples of left ventricular hypertrophy and remodeling in specific groups. Representative midventricular sections of the left ventricle stained with trichrome-Masson are shown. ShamC: control sham group, ShamM: metformin-treated sham group, ARC: untreated AR group and ARM: metformin-treated AR group. Scale bar at the bottom right of the figure: 1cm.

Figure 3: Metformin treatment effects on stroke volume and cardiac output as evaluated by echocardiography. Results are reported in % of change relative to the untreated control sham group (SC) as mean ± SEM (n = 13–15/group). Two-way ANOVA statistical analysis results are displayed below each graph. D X T: disease and metformin treatment interaction *: $p<0.05$ vs. untreated corresponding group from Bonferroni post-test if $P<0.05$ for D x T.

Figure 4: Up-regulation of hypertrophy markers in AR animals. LV mRNA levels of atrial natriuretic peptide (ANP), brain natriuretic peptide (BNP), endothelin-1 (ET-1) and c-Fos were evaluated as described in the Material and methods section. Results are reported in arbitrary units as mean ± SEM (n = 13–15/group). Untreated sham (sham operated animals) group mRNA levels were normalized to 1. Two-way ANOVA statistical analysis results are displayed below each graph. D X T: disease and metformin treatment interaction.

Figure 5: Evaluation by real-time quantitative RT-PCR of the LV mRNA levels of genes related to extracellular matrix remodeling. Results are reported as mean ± SEM (n=10-15/gr). ColI: collagen I; ColIII: collagen III; ColIV Fn: fibronectin; LOX1: lysyl oxidase 1; TGFb1: transforming growth factor;, MMP2: matrix metalloprotease 2 and TIMP-1: tissue inhibitor of metalloprotease 1. Two-way ANOVA statistical analysis results are displayed below each graph. D X T: disease and metformin treatment interaction *: $p<0.05$ vs. untreated corresponding group from Bonferroni post-test if $P<0.05$ for D x T.

Figure 6: Activity levels of enzymes implicated in myocardial energy metabolism. HADH (hydroxyacyl-Coenzyme A dehydrogenase), HK (hexokinase) and CS (citrate synthase) enzymatic activities were measured in LV homogenates from at least 10 animals in each group as described in the Materials and Methods. Results are reported as mean ± SEM (n=10-15/gr). Two-way ANOVA analyses are displayed below each panel. D X T: disease and metformin treatment interaction.

Figure 7: Evaluation by real-time quantitative RT-PCR of the LV mRNA levels of genes related to cardiac metabolism. Glucose transporters 1 and 4 (Glut1 and Glut4), fatty acid transporter (FAT/CD36), carnityl palmitoyl transferases (Cpt 1b and 2), PDK4 (pyruvate dehydrogenase kinase 4) PDH1a (pyruvate dehydrogenase 1alpha), MCAD (medium-chain acyl-CoA dehydrogenase), UCP3 (uncoupling protein 3), DGKζ (diacylglycerol kinase ζ), Ant1 (adenine nucleotide transferase 1), PPARα (peroxisome proliferator-activated receptor α) and PGC1α (peroxisome proliferator-activated receptor gamma coactivator-1α). Results are reported in arbitrary units as mean ± SEM (n = 10/group). Untreated sham (sham-operated animals; SC) group mRNA levels were normalized to 1 and are represented by the black lane. *: $p<0.05$ vs. ARC group.

Figure 8: MAP kinases, LKB1, AMP kinase and Akt levels of activation in AR rats treated or not with metformin. Evaluation of the phosphorylated and the total protein contents for each signaling molecules were performed by immunoblotting as described in the Materials and methods section. Results are reported in arbitrary units as mean ± SEM (n=10–12/group) of the ratio of the phosphorylated content on the total protein content. Untreated sham (sham-operated animals; SC) group protein contents were normalized to 1 and are represented by the black lane. *: $p<0.05$ vs. ARC group.

Table 1: QuantiTect® Primer Assays used in Q-PCR analysis of gene expression.

mRNA	Symbol	Accession No.	Catalog No.	Amplicon (bp)
acyl-Coenzyme A dehydrogenase, C-4 to C-12 straight chain	MCAD	NM_016986	QT01081871	124
carnitine palmitoyltransferase 1b, muscle	Cpt1b	NM_013200	QT01084069	98
carnitine palmitoyltransferase 2	CPT2	NM_012930	QT00186473	150
Endothelin-1	Edn1	NM_012548	QT00371308	60
Fatty acid translocase/CD36	FAT/CD36	XM_575338	QT01702680	81
Fibronectin 1	Fn1	NM_019143	QT00179333	92
Lysyl oxidase	Lox	NM_017061	QT00185591	148
matrix metallopeptidase 2	Mmp2	NM_031054	QT00996254	103
Natriuretic peptide precursor A	ANP	NM_012612	QT00366170	107
Natriuretic peptide precursor B	BNP	NM_031545	QT00183225	94
osteosarcoma viral oncogene homolog	Fos	NM_022197	QT01576330	73
peroxisome proliferator activated receptor alpha	PPARalpha	NM_013196	QT00176575	66
PPAR gamma, coactivator 1 alpha	PGC1alpha	NM_031347	QT00189196	108
Procollagen-1 alpha-1	ColI	NM_053304	QT00370622	92
Procollagen-3 alpha-1	ColIII	NM_032085	QT01083537	111
Procollagen-4 alpha-1	ColIV	NM_001135009	QT00005250	119
Pyruvate dehydrogenase alpha 1	PDHa1	NM_001004072	QT01830220	93
Pyruvate dehydrogenase kinase, isozyme 4	Pdk4	NM_053551	QT00189287	145
solute carrier family 2 member 1	GLUT1	NM_138827	QT00178024	85
solute carrier family 2 member 4	GLUT4	NM_012751	QT00175931	146
solute carrier family 25, member 4	ANT1	NM_053515	QT01081633	143
Tissue inhibitor of metallopeptidase 1	Timp1	NM_053819	QT00185304	113
Transforming growth factor beta 1	Tgfbeta1	NM_021578	QT00187796	145
Uncoupling protein 3	UCP3	NM_013167	QT00176589	103

Table 2. Animal characteristics.

Parameters	SC (14)	SM (13)	ARC (11)	ARM (16)	Disease	Treatment	D x T
					P value	P value	P value
Body Weight, g	568 ± 9.9	580 ± 9.4	548 ± 5.3	552 ± 6.4	0.0047	0.34	0.69
Tibial length, mm	58 ± 0.5	58 ± 0.4	58 ± 0.4	58 ± 0.4	0.31	0.32	0.72
Heart, mg	1206 ± 42.0	1180 ± 30.7	1988 ± 58.2	1911 ± 31.4	<0.0001	0.22	0.54
LV, mg	875 ± 28.5	843 ± 19.4	1487 ± 55.4	1432 ± 26.9	<0.0001	0.22	0.75
RV, mg	231 ± 8.7	229 ± 7.0	340 ± 16.6	319 ± 7.9	<0.0001	0.28	0.36

SC: sham control (untreated), SM: sham metformin-treated animals, ARC, aortic regurgitation control group and ARM: aortic regurgitation metformin-treated animals. LV: left ventricle and RV: right ventricle. Values are expressed as mean ± SEM. The number of animals per group is indicated in parenthesis. P values from 2-way ANOVA analysis are shown on the right to evaluate separately the general impact of the disease or the metformin treatment and the interaction between disease and treatment (D x T).

Table 3. Echocardiography data.

Parameters	SC	SM	ARC	ARM	Disease	Treatment	D x T
					P value	P value	P value
EDD, mm	7.6 ± 0.09	6.9 ± 0.14[b]	10.5 ± 0.19	9.1 ± 0.18[c]	<0.0001	<0.0001	0.042
ESD, mm	3.5 ± 0.11	3.1 ± 0.08	6.4 ± 0.27	4.9 ± 0.29[c]	<0.0001	<0.0001	0.0046
SW, mm	1.2 ± 0.02	1.4 ± 0.03	1.2 ± 0.04	1.4 ± 0.03	0.92	<0.0001	0.074
PW, mm	1.2 ± 0.04	1.3 ± 0.02	1.2 ± 0.05	1.3 ± 0.02	0.81	0.002	0.61
RWT	0.32 ± 0.008	0.39 ± 0.012	0.23 ± 0.006	0.30 ± 0.008	<0.0001	<0.0001	0.84
EF, %	78 ± 1.2	78 ± 1.2	62 ± 2.2	72 ± 2.4[b]	<0.0001	0.017	0.017

SC: sham control (untreated), SM: sham metformin-treated animals, ARC, aortic regurgitation control group and ARM: aortic regurgitation metformin-treated animals. EDD: end-diastolic diameter, ESD: end-systolic diameter, SW: septal wall thickness, PW: posterior wall thickness, RWT: relative wall thickness, EF: ejection fraction. Measurements obtained under 1.5% isoflurane anesthesia. Values are expressed as mean ± SEM. The number of animals per group is indicated in parenthesis. P values from 2-way ANOVA analysis are shown on the right to evaluate separately the general impact of the disease or the metformin treatment and the interaction between disease and treatment (D x T). b: $p<0.01$ and c: $p<0.001$ vs. untreated corresponding group from Bonferroni post-test if $P<0.05$ for D x T.

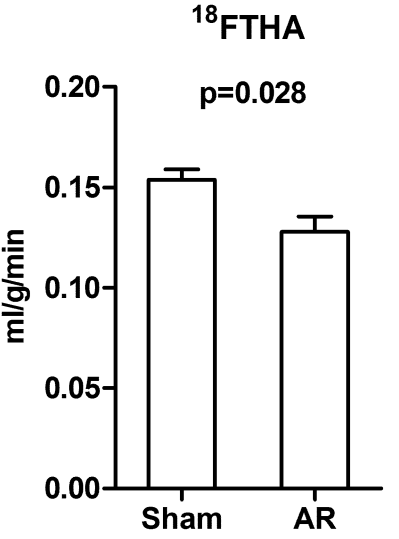
18FTHA
p=0.028
0.20
0.15
0.10
0.05
0.00
ml/g/min
Sham
AR

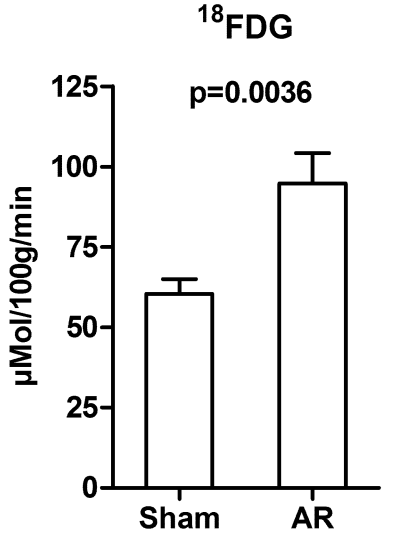
18FDG
p=0.0036
125
100
75
50
25
0
µMol/100g/min
Sham
AR

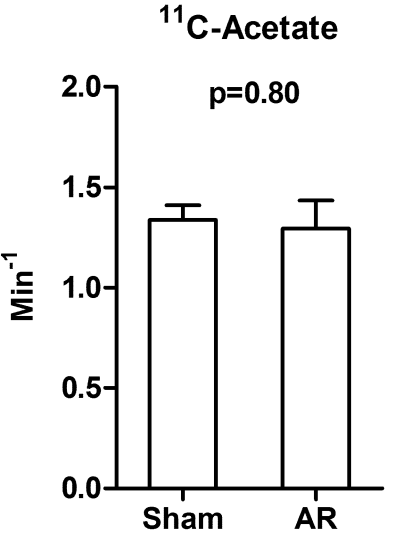
11C-Acetate
p=0.80
2.0
1.5
1.0
0.5
0.0
Min-1
Sham
AR

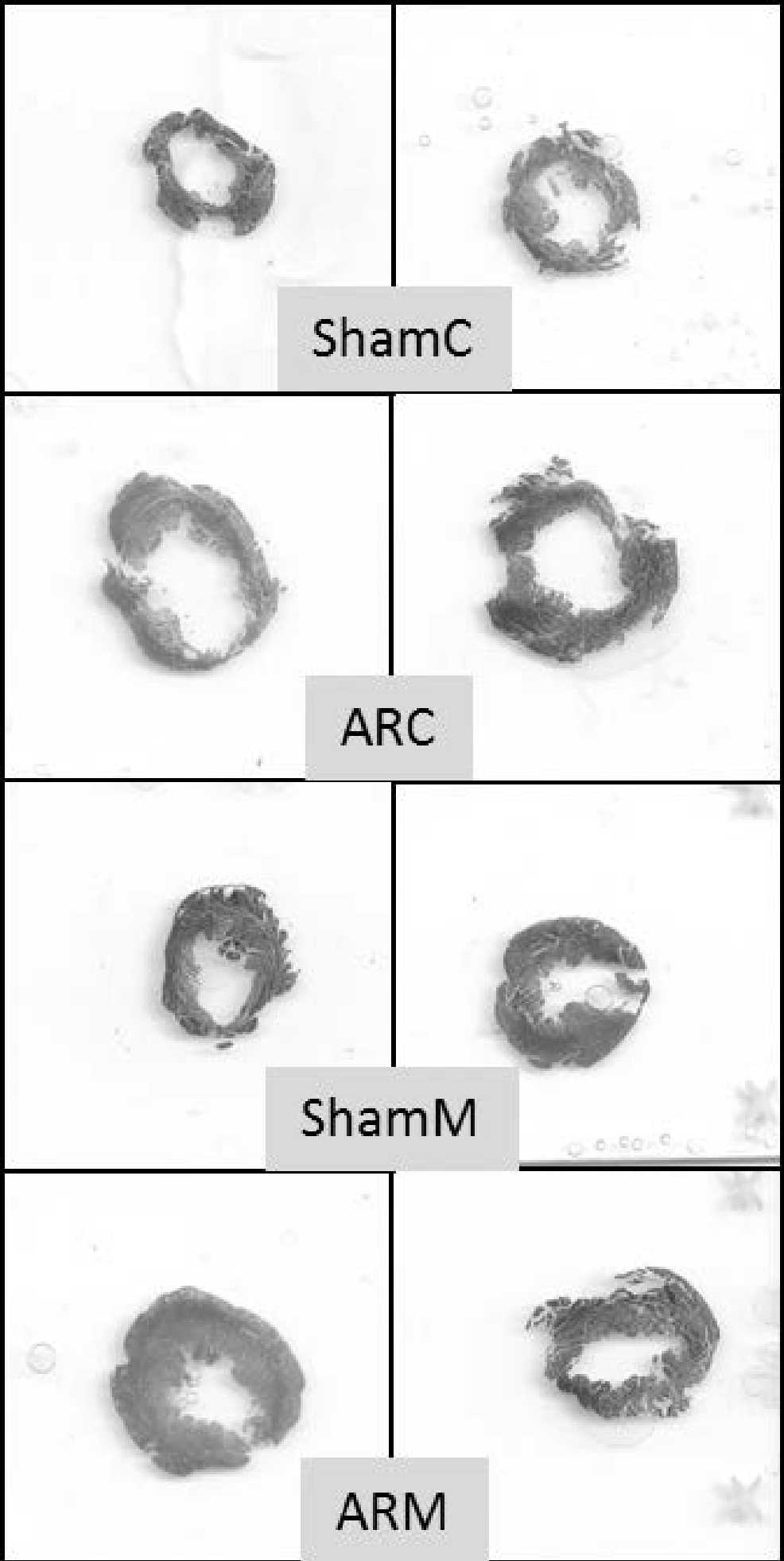
ShamC
ARC
ShamM
ARM

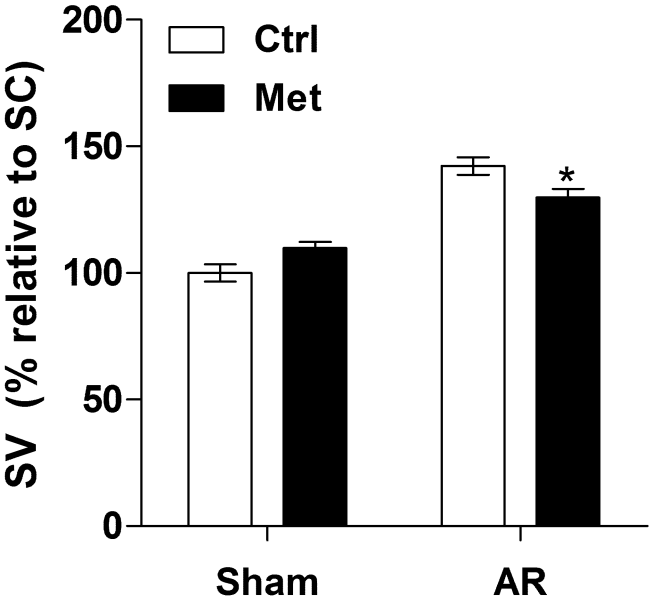

Disease	<0.0001
Treatment	0.70
D X T	0.011

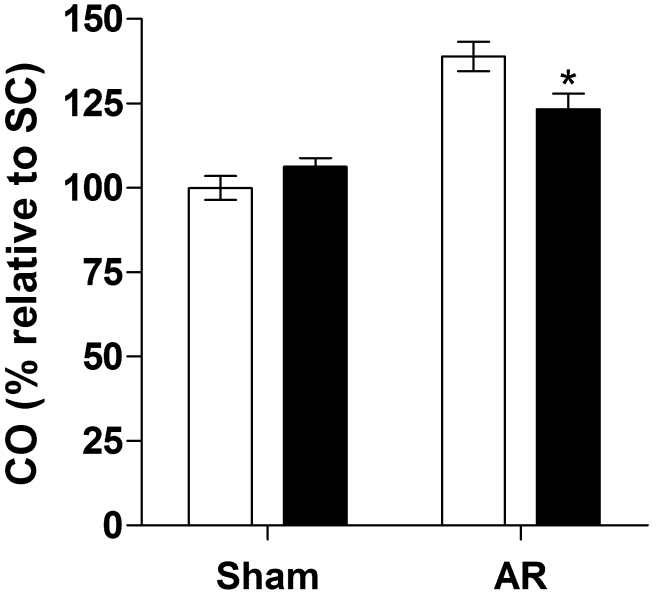

Disease	<0.0001
Treatment	0.24
D X T	0.0075

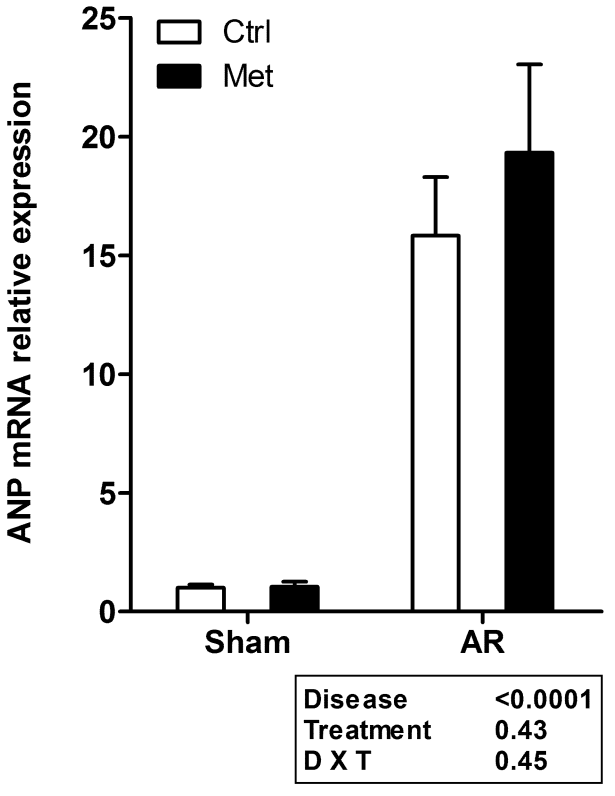
Ctrl
Met
ANP mRNA relative expression
25
20
15
10
5
0
Sham
AR
Disease <0.0001
Treatment 0.43
D X T 0.45

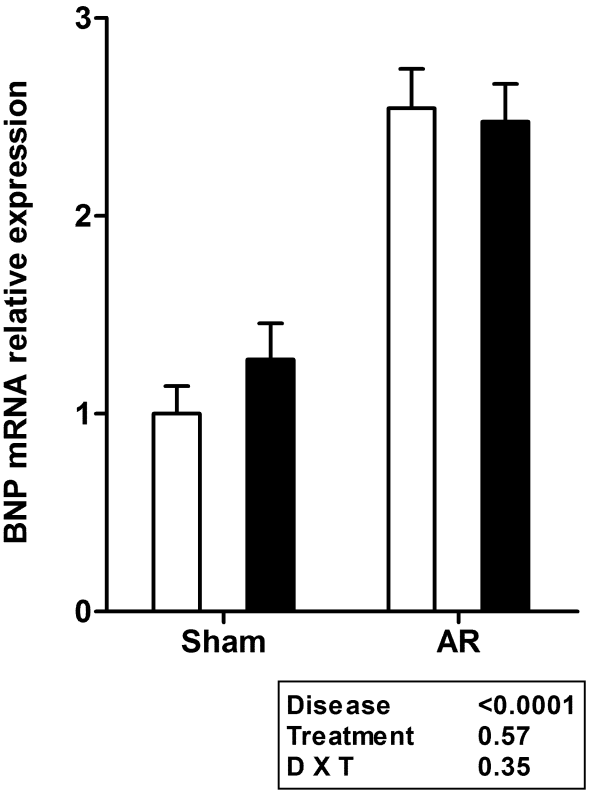
BNP mRNA relative expression
3
2
1
0
Sham
AR
Disease <0.0001
Treatment 0.57
D X T 0.35

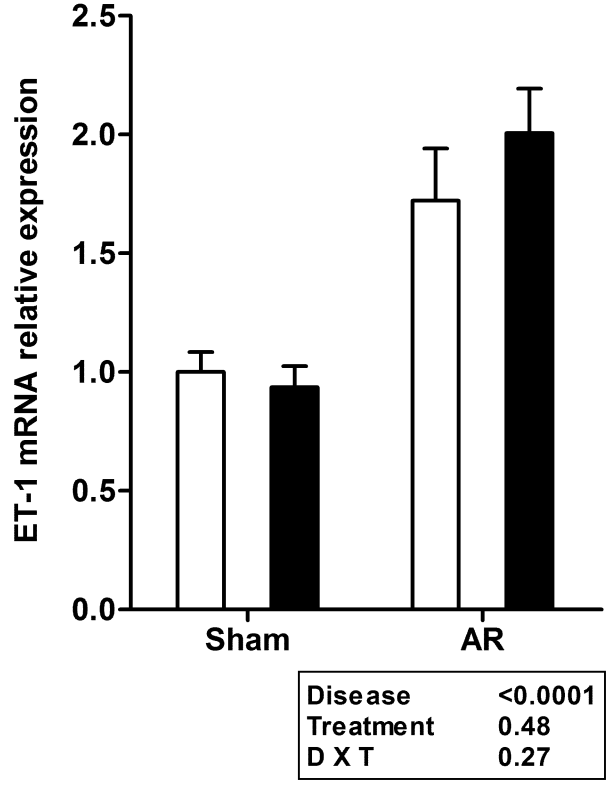
ET-1 mRNA relative expression
2.5
2.0
1.5
1.0
0.5
0.0
Sham
AR
Disease <0.0001
Treatment 0.48
D X T 0.27

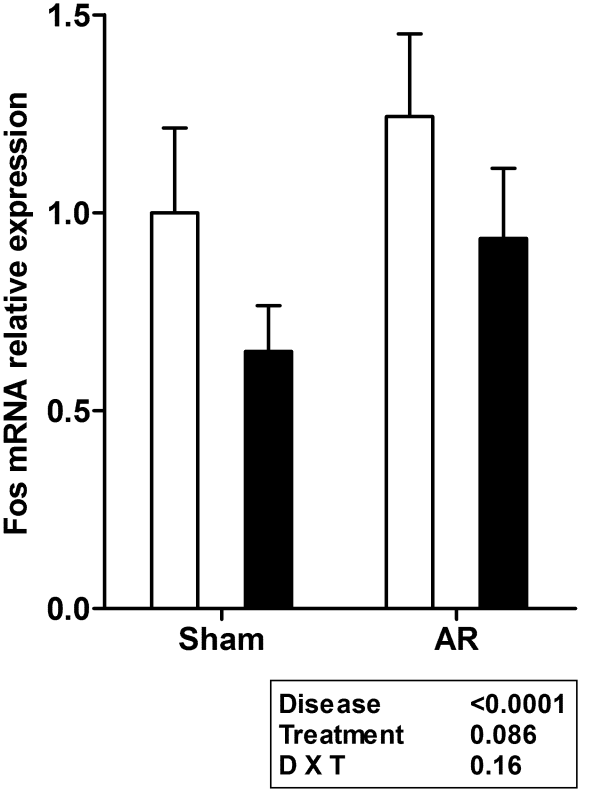
Fos mRNA relative expression
1.5
1.0
0.5
0.0
Sham
AR
Disease <0.0001
Treatment 0.086
D X T 0.16

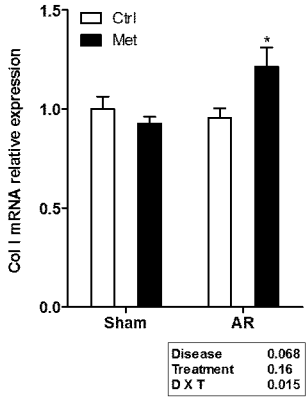

Disease	0.068
Treatment	0.16
D X T	0.015

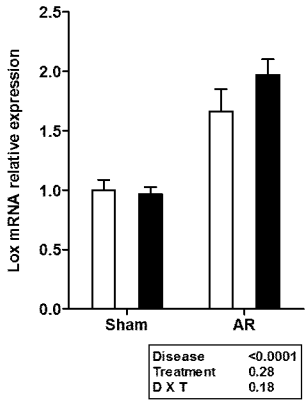

Disease	<0.0001
Treatment	0.28
D X T	0.18

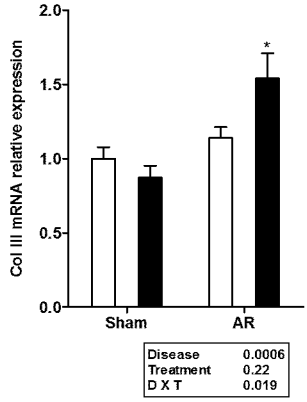

Disease	0.0006
Treatment	0.22
D X T	0.019

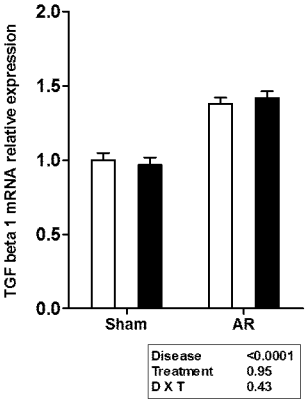

Disease	<0.0001
Treatment	0.95
D X T	0.43

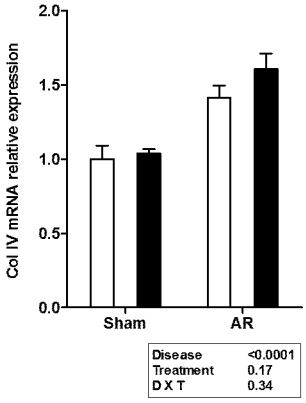

Disease	<0.0001
Treatment	0.17
D X T	0.34

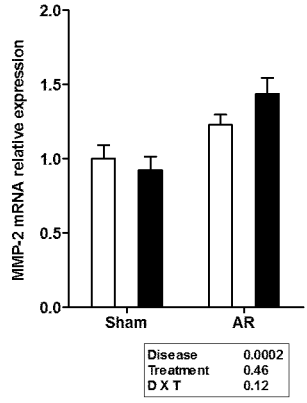

Disease	0.0002
Treatment	0.46
D X T	0.12

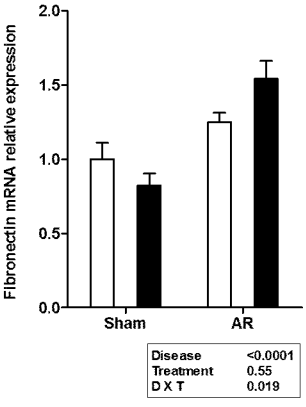

Disease	<0.0001
Treatment	0.55
D X T	0.019

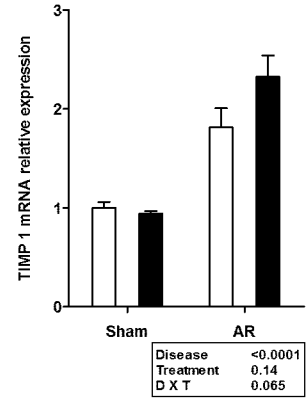

Disease	<0.0001
Treatment	0.14
D X T	0.065

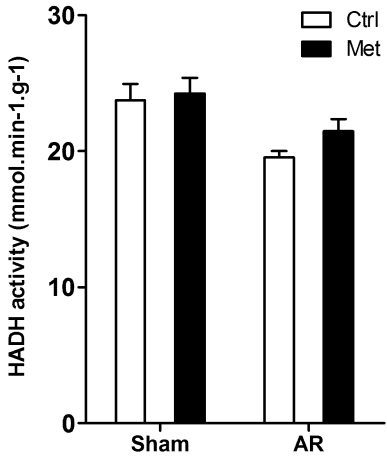

Disease	0.0009
Treatment	0.22
D X T	0.45

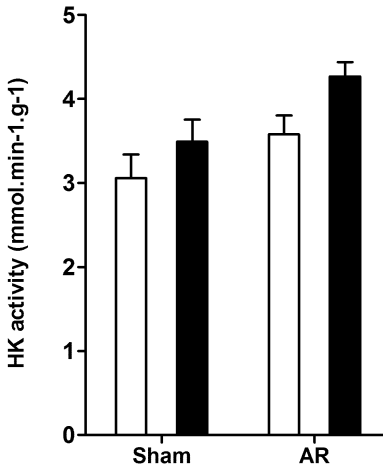

Disease	0.025
Treatment	0.010
D X T	0.60

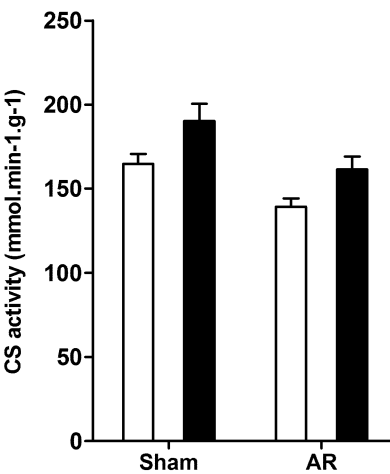

Disease	0.0006
Treatment	0.0023
D X T	0.83

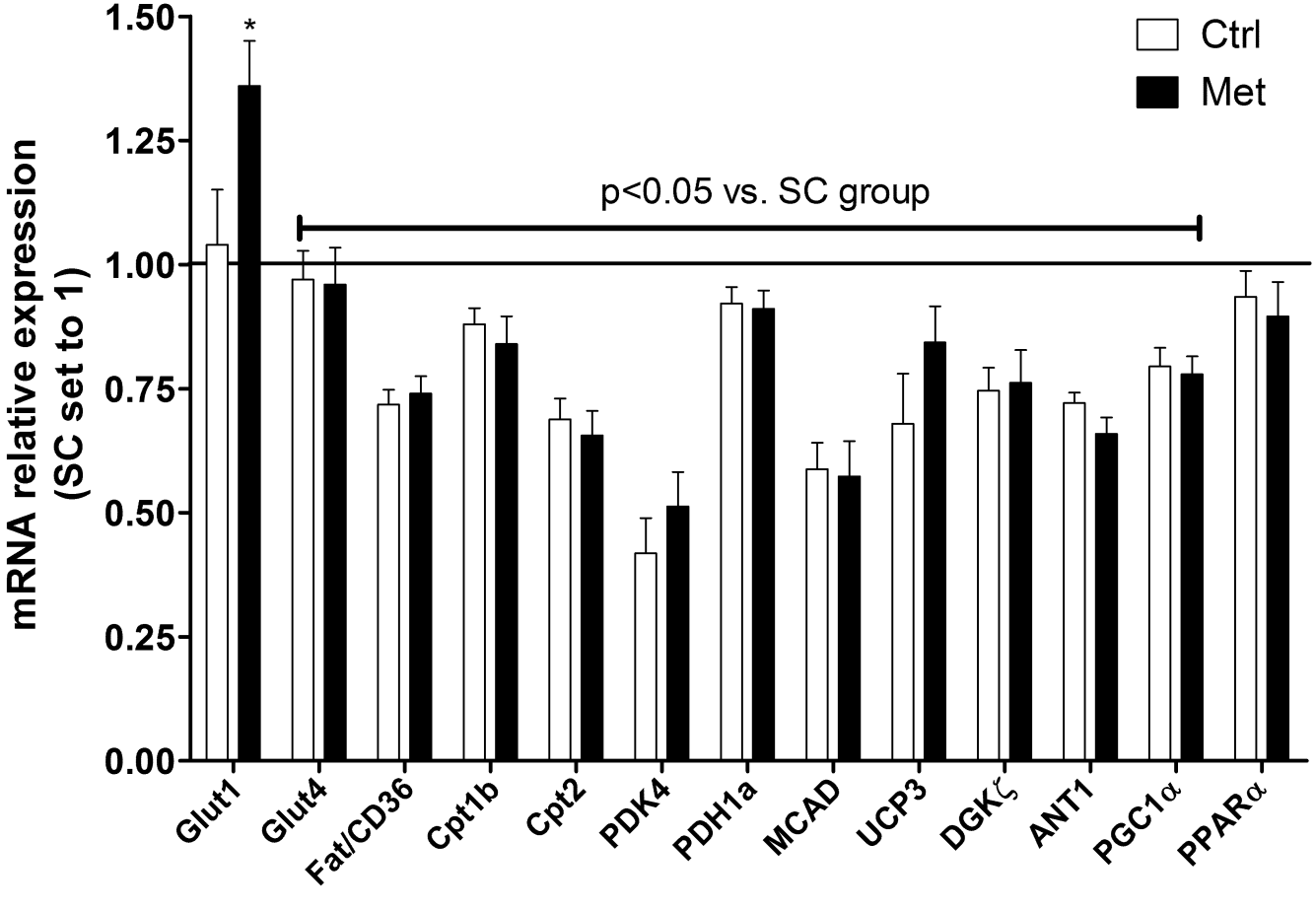
1.50
1.25
1.00
0.75
0.50
0.25
0.00
mRNA relative expression
(SC set to 1)
Ctrl
Met
*
p<0.05 vs. SC group
Glut1
Glut4
Fat/CD36
Cpt1b
Cpt2
PDK4
PDH1a
MCAD
UCP3
DGKζ
ANT1
PGC1α
PPARα

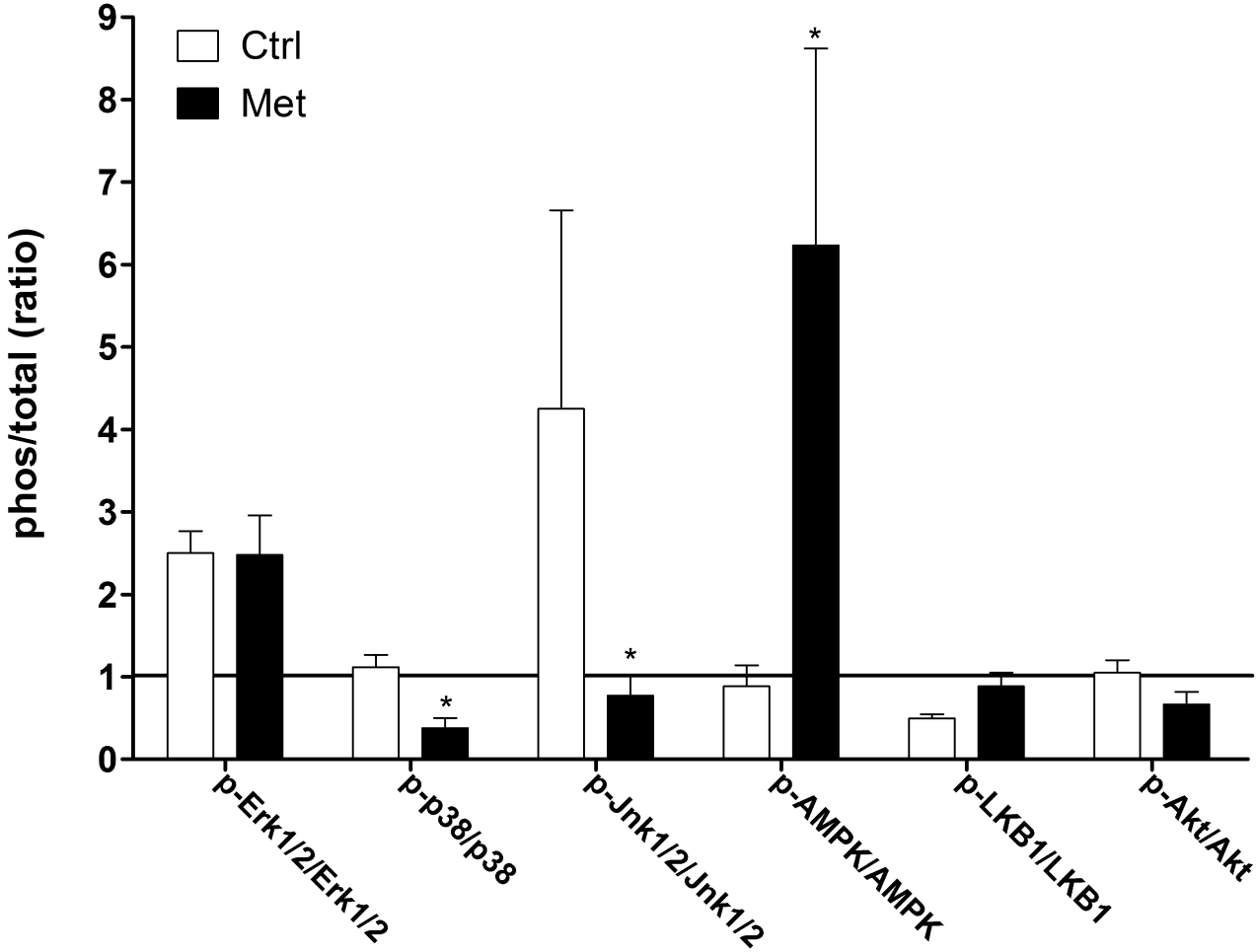
Ctrl
Met
phos/total (ratio)
0
1
2
3
4
5
6
7
8
9
*
*
*
p-Erk1/2/Erk1/2
p-p38/p38
p-Jnk1/2/Jnk1/2
p-AMPK/AMPK
p-LKB1/LKB1
p-Akt/Akt